

# TransAT Report Series

– Presentations –

## The *CMFD* code TransAT

Phase-Change Heat Transfer

ASCOMP Switzerland

Edited by: Djamel Lakehal

Release date: Sep, 2014

References: TRS-P/ 04-2014

# AT

## Table of Contents

Table of Contents .....	2
1. Introduction .....	3
2. Phase-Average Modelling of Phase Change.....	3
2.1. Transport Equations in the Phase-Average Approach.....	3
2.2. Wall Boiling Model .....	4
3. Direct Simulation of Phase Change .....	5
3.1. Transport Equations .....	5
3.2. Interfacial Mass Transfer: Approach 'A' .....	6
3.3. Interfacial Mass Transfer: Approach 'B' .....	6

**Abstract:**

This note describes the multiphase flow models and strategies implemented in the CFD/CMFD code TransAT.

**1. Introduction**

Heat transfer featuring phase change has enormous importance in industrial processes, including heat exchangers, electronics cooling and thermal hydraulics of nuclear power plants. Because of its wide applications, a general modelling capability for predicting nucleate and convective boiling within a modern CMFD code is desirable and remains the objective of many researchers. Boiling occurs as nucleate, transition and film boiling. Compared to film boiling, nucleate boiling is more efficient in heat removal, which makes it potentially useful for thermal management in high density power electronics. Advanced electronic systems require today tailored heat removal techniques that can deal with heat fluxes as high as 10 MW/in<sup>2</sup>. Thermal systems based on single-phase liquid loops are close to their maximum heat removal capability and will no longer satisfy the increasing thermal demands of new applications.

The mainstream modelling approach for multiphase flow systems involving phase-change heat transfer is based on the Eulerian-Eulerian, two-fluid model, which requires closure laws for the phase-to-phase and wall-to-flow mass, momentum, and energy terms in the governing equations. Subcooled boiling heat transfer is captured by the wall-to-flow constitutive relation for energy. Examples of mechanistic boiling heat transfer models are the heat flux partitioning model of Kurul and Podowski (1990) and its recent modified variant (Krepper et al. (2001)). TransAT incorporates this modelling strategy within its phase-average N-phase model, as well as advanced phase-change modelling based on interface tracking (Level Set Method).

**2. Phase-Average Modelling of Phase Change****2.1. Transport Equations in the Phase-Average Approach**

Phase-average models for multiphase flow approaches could be used under the two-fluid, six equation formulation or the homogeneous mixture model, with or without drift or slip, which is determined algebraically in contrast to the two-fluid variant. Phase change is incorporated in the transport equation virtually in the same way: there is no direct integration of heat fluxes near the interface or near the wall, rather, a mass transfer model is prescribed based in experiments, or on DNS; the latter is still less generalized. The two-fluid model equations are well known in the literature and thus are not introduced here. The reader may refer to various papers for details. The Eulerian multiphase (phase-average) model under its 'original' homogeneous form could be used to capture the evolution of the two phases with heat transfer. The vapour phase is modelled as the secondary phase in the primary liquid flow. Under the original homogeneous form of the Eulerian model where the drift or slip velocity  $u_D$  is set to zero, the conservation equations are solved for the mixture quantities, including density, viscosity, velocity (denoted hereinafter as  $u_m$  and sometimes as  $V_m$ ), pressure and temperature, and phase volume fractions defined as:

$$\mathbf{u}_m = \sum_{k=G,L} \frac{\alpha_k \rho_k \mathbf{u}_k}{\alpha_k \rho_k}; \rho_m = \sum \alpha_k \rho_k \quad (1)$$

$$Y_k = \alpha_k \rho_k / \rho_m; \mathbf{u}_D = \mathbf{u}_G - \mathbf{u}_m$$

For bubbly flows, the simplest model for the drift velocity can be defined by:

$$u_{Dj} = \frac{2 \alpha_L R_b^2 (\rho_G - \rho_L)}{9 \alpha_G \mu_m} Y_L (Y_L - \alpha_L) \frac{\partial p}{\partial x_j} \quad (2)$$

In the N-Phase approach extending the original two-phase mixture model, we have modified the original formulation such that the energy is solved for each phase to better cope with interphase mass transfer, whereas the momentum is solved for the mixture; here the pressure is also taken for mixture. Further, the model could be used in TransAT either under this homogeneous form or by adding an algebraic slip velocity to separate the phases. The final form of the governing equations system under homogeneous assumption reads (where subscript k denotes each phase):

$$\frac{\partial}{\partial t}(\alpha_k \rho_k) + \frac{\partial}{\partial x_j}(\alpha_k \rho_k V_{jk}) = \dot{m} \quad (3)$$

$$\frac{\partial}{\partial t}(\rho^m V_i^m) + \frac{\partial}{\partial x_j}(\rho^m V_i^m V_j^m) = -\frac{\partial}{\partial x_i} p^m + \frac{\partial}{\partial x_j}(2\mu^m S_{ij}^m) + \rho^m g \quad (4)$$

$$\frac{\partial}{\partial t}(\rho_k C_{pk} T_k) + \frac{\partial}{\partial x_j}(\rho_k C_{pk} T_k V_{jk}) = \frac{\partial}{\partial x_j} \left( \lambda_k \frac{\partial T_k}{\partial x_j} \right) + q_w \quad (5)$$

where the superscript m indicates the phase-averaged quantities,  $V_{ik}^D = V_{ik} - V_i^m$  is the drift velocity of each phase k,  $\dot{m}$  is the mass-transfer rate, and  $q_w$  is the heat flux due to phase change. In the algebraic slip extension of the model, additional slip-induced convection and diffusion fluxes appear in Eq. (2). In the algebraic slip extension of the model, additional slip-induced convection and diffusion fluxes appear in Eq. (5).

## 2.2. Wall Boiling Model

As mentioned earlier, the wall heat flux ( $q_{wall}$  [W/m<sup>2</sup>]) is partitioned into three parts:

$$q_{wall} = q_f + q_q + q_e \quad [W/m^2] \quad (6)$$

The first part is the single-phase heat transfer (convective heat flux):

$$q_f = A_1 St_p \rho_l C_{pl} u_{lp} (T_{wall} - T_l); \quad A_1 = 1 - A_2 \quad (7)$$

where  $A_1$  and  $A_2$  represent the fraction of the wall surface influenced by liquid and by vapour bubbles formed on the wall, respectively,  $T_l$  and  $u_{lp}$  are the liquid temperature and velocity at the cell adjacent to the wall,  $C_{pl}$  is the liquid heat capacity, and  $St_p$  is the Stanton number  $St_p = Nu / (Re_l Pr_l)$ . Various correlations for the Nusselt number  $Nu$  exist in the literature. For the present formulation, we resort to the selection procedure employed by Vyskocil and Macek (2008):

$$Nu = \max \left( \sqrt{\frac{4Pe}{\pi}}, \frac{12}{\pi} Ja, 2 \right) \quad (8)$$

where  $Pe$  and  $Ja$  denote the Peclet and Jacob numbers, respectively. The second part of the wall heat flux is attributed to the quenching mechanism and is defined by:

$$q_q = A_2 \alpha_{quench} (T_{wall} - T_l); \quad A_2 = \min(0.25 \cdot \pi \cdot d_w^2 \cdot n, 1) \quad (9)$$

where  $\alpha_{quench}$  is the associated heat transfer coefficient,  $d_w$  is the bubble departure diameter calculated using Ůnal's (1976) correlation, and n is the active nucleation site density determined using the correlation of Eddington and Kenning (1979) given by,

$$n = (210 \cdot (T_{wall} - T_{sat}))^{1.8} \left[ \frac{1}{m^2} \right] \quad (10)$$

The portion of heat flux due to liquid evaporation ( $q_e = \dot{m}_e \cdot h_{fg}$ ), in which  $h_{fg}$  denotes the latent heat of phase change, involves two additional unknowns: namely the bubble detachment frequency  $f$  and the active nucleation site density  $n$  defined above:

$$m_e = \frac{\pi \cdot d_w^3}{6} \rho_v \cdot f \cdot n \quad \left[ \frac{kg}{m^2 s} \right] \quad (11)$$

$$f = \sqrt{\frac{4 \cdot g \cdot (\rho_l - \rho_v)}{3 \cdot d_w \cdot \rho_l}} \quad \left[ \frac{1}{s} \right] \quad (12)$$

The quenching heat transfer coefficient  $\alpha_{quench}$  quench is dependent on the waiting time  $t_w$  between the bubble departure and the next bubble formation period ( $t_w = 1/f$ ):

$$\alpha_{quench} = 2 \cdot \lambda_l \cdot f \cdot \sqrt{\frac{t_w}{\pi \cdot a_l}} \quad \left[ \frac{W}{m^2 K} \right] \quad (13)$$

The cubic dependence in Eq. (11) suggests that small uncertainties on the bubble departure diameter are greatly magnified in the heat transfer model, thus deteriorating the accuracy of the overall CFD simulation. Therefore, using more accurate bubble departure models are key to the successful prediction of subcooled flow boiling heat transfer.

### 3. Direct Simulation of Phase Change

#### 3.1. Transport Equations

Interfacial flows refer to multi-phase flow problems that involve two or more immiscible fluids separated by sharp interfaces which evolve in time. Typically, when the fluid on one side of the interface is a gas that exerts shear (tangential) stress upon the interface, the latter is referred to as a free surface. ITM's are best suited for these flows, because they represent the interface topology rather accurately. The single-fluid formalism solves a set of conservation equations with variable material properties and surface forces Lakehal et al. (2002).

The incompressible multifluid flow equations within the single-fluid formalism read:

$$\nabla \cdot \mathbf{u} = 0 \quad (14)$$

$$\partial_t(\rho \mathbf{u}) + \nabla \cdot (\rho \mathbf{u} \mathbf{u}) = -\nabla p + \nabla \cdot \boldsymbol{\tau} + \mathbf{F}_s + \mathbf{F}_g \quad (15)$$

where  $\mathbf{F}_g$  is the gravitational force,  $F_s$  is the surface tension force, with  $\mathbf{n}$  standing for the normal vector to the interface.

To track the interface separating two immiscible phases and update material properties, a topology equation is solved for the level-set function  $\phi$ :

$$\frac{\partial \phi}{\partial t} + \mathbf{u} \cdot \nabla \phi = \dot{m} / \rho |\nabla \phi| \quad (16)$$

where the phase change due to heat transfer is accounted for by the source term;  $\dot{m}$  being the rate of mass transfer. In the Level Set technique used in TransAT, the interface between immiscible fluids is represented by a continuous function  $\phi$ , representing the distance to the interface that is set to zero on the interface, is positive on one side and negative on the other.

### 3.2. Interfacial Mass Transfer: Approach 'A'

The jump conditions across a steam-water interface are schematically drawn in Fig. 1 shown next. The scheme shows that the most important jump in terms of quantity is the mass flux or rate of mass transfer. The jump on temperature and pressure is generally only indirectly accounted for by assigning the temperature at the interface to saturation ( $T_{g,i} = T_{l,i} = T_{sat}$ ). Further, only a few authors make  $T_{sat}$  in effect dependent on  $P_{sat}$ . What we refer to here as 'Approach A' is the direct technique in which the rate of mass transfer  $\dot{m}$

$$\dot{m}h_{l,v} = (\lambda_L \nabla T_L - \lambda_v \nabla T_v) \quad (17)$$

is directly integrated across the interface (Lakehal et al., 2002) using the energy jump across the interface. With this approach, in contrast to phase averaged models; there is no need to determine an interfacial area.

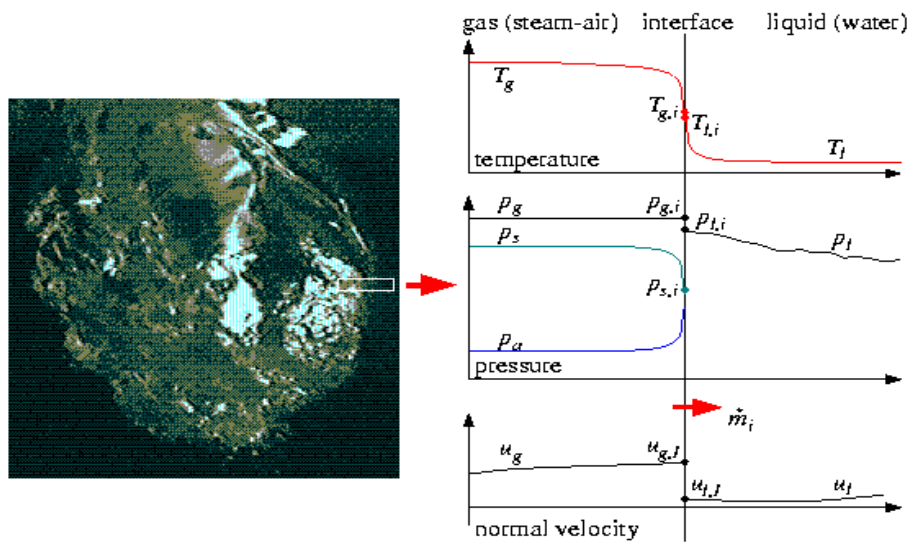


Figure 1: Schematic of interfacial jump conditions at a steam-water interface.

Thermal gradients on both sides of the interface are resolved on the grid. This is possible for some cases only where the interfacial thermal sublayer is within reach of the specified grid. For example, use of this approach to predict the departure and growth of a single bubble under low-to-medium heat flux is possible. In case the heat flux is high, the mass transfer rate is forced to be active only at the triple line as a source term applied only in the cell containing the triple line. In this latter case the mass transfer rate is not directly resolved but fixed by reference to a model, albeit the interface motion is directly calculated using ITMs. Note that the combination of the above model for wall boiling and interfacial phase change is possible but requires further developments. Note, too, that the implementation details are quite cumbersome using this technique and only a few successful cases have been reported in the literature.

### 3.3. Interfacial Mass Transfer: Approach 'B'

We refer to here, as 'Approach B' the strategy amounting at specifying an interfacial heat transfer model that depends on some local or global variables. This approach is used when 'Approach A' is not capable to resolve the interfacial layer with the required details. This is generally the case for turbulent interfacial gas-liquid flows featuring massive interfacial changes and a high interfacial heat flux. Transport models for turbulent phase-change heat transfer have been borrowed from equivalent mass transfer models for high Schmidt numbers,  $Sc \gg 1$ . Briefly, the models can be divided into two major classes: those based on the turbulent diffusivity concept, and those based on the eddy model concept. In the first class of

models, turbulent transport is embedded into turbulent diffusivity made proportional to the distance to the interface and inversely proportional to the turbulence time-scale beneath the interface. In the second class, the transport is associated to the periodical renewal of fluid elements occurring at the interface (i.e. the surface renewal theory of Higbie (1935)). Here, the key is the determination of the relationship between the interfacial turbulence characteristics and the so-called "contact time", which is the typical time that an eddy spends in contact with the interface. With either approach, the problem reduces to estimating the characteristic time-scale associated with the turbulent interfacial eddies that control the transport.

Interfacial heat transfer correlations based on the eddy model concept can be expressed in terms of transfer velocity ( $K$  [m/s]), or in terms of dimensionless heat transfer numbers (Nusselt number:  $Nu$ ), based on non-dimensional numbers relevant to the fluid and flow nature, i.e. bulk Reynolds number, turbulent Reynolds number and Prandtl number  $Pr$ :

$$K_L^+ = Re_t^m Pr_L^n ; Nu_L = Re_G^p (or Re_t^p) Re_G^q Pr_L^l \quad (18)$$

Use is made of steam-water transfer models, expressed either in terms of  $K+$  or  $Nu$ . Several other forms of parameterization were suggested. The heat transfer velocity can be scaled with the turbulence velocity-scale  $u_t$ , the interfacial frictional velocity  $U_t = (\rho\tau_{int})^{1/2}$ , or the turbulence intensity  $v'$ .

In practice, however, the implementation of these models is made complicated because of the lack of an appropriate definition of the turbulent Reynolds number  $Re_t = L_t u_t / \nu_L$ , in which  $L_t$  stands for the characteristic length scale. In the RANS context, the length and velocity scales of turbulence  $L_t$  and  $u_t$  are often made proportional to  $kL$  and  $\varepsilon L$ , the turbulent kinetic energy (TKE) and its rate of dissipation. In fact, the turbulent characteristics velocity and length-scale should depend on whether use is made of RANS or LES and alternatively V-LES. Further, while in the two-fluid formulations, use is generally made of Nusselt number, since the models cope with phase change using the heat transfer coefficient (HTC)

$$h_L = Nu_L \lambda_L / L_t,$$

in ITMs, however, use is rather made of  $K+$  since the approach requires the definition of a transfer velocity  $K = \dot{m} / \rho$  [m/s], with  $\dot{m}$  is the rate of interfacial mass transfer [kg/m<sup>2</sup>.s]. The interfacial heat flux is determined there using

$$q_L'' = h_L (T_{int} - T_{sat}),$$

with HTC being determined using the model (in terms of  $Nu$  or  $K+$ ), where indices 'int' and 'sat' for temperature 'T' refer to interfacial and saturation, respectively. For the contribution of small-scale energy dissipative eddies, use is made of the Kolmogorov velocity and length scales, respectively. In SD model, the DNS-based correlation for the heat transfer rate takes the following form:

$$K / u_t \equiv \dot{m} / \rho \cdot u_t = C \cdot Pr^n \cdot f [Re_t] Re_t^m \quad (19)$$

where the model constant  $C$  depends on the liquid properties:  $C = 0.35$  for  $Pr = 1$ , and  $= 0.45$  for  $Pr \gg 1$ ), and Schmidt/Prandtl and turbulence Reynolds number exponents 'n' and 'm' are governed by the surface condition and turbulence intensity. The difference between the SD and the so-called 'Small-Eddy' and 'Large-Eddy' models is the presence of the function between brackets in Eq. (19), known as the surface-divergence function. This has previously

been modelled using DNS data for both passive scalar transfers (Banerjee et al., 2004), and recently for active condensing flow (Lakehal et al., 2008, Lakehal et al., 2008):

$$f [ Re_t ] = \left[ 0.3 \left( 2.83 Re_t^{3/4} - 2.14 Re_t^{2/3} \right) \right]^{1/4} \quad (20)$$

In the ‘Small-Eddy’ models, exponent ‘m’ in (19) is set to -1/4, while in the ‘Large-Eddy’ variant, ‘m’ is equal to -1/2; in the original form of both models, the surface divergence function (Eqn. 20) is set to unity. As to the Prandtl number exponent ‘n’, it takes the value of -1/2 for free surfaces and about -2/3 for surfaces behaving like rigid walls. The ‘SD Scale-Adaptive’ model implemented in TransAT borrows the ‘two-regime’ idea from Theophanous et al (1976) and blends the exponent ‘m’ in (19) between -1/4 and -1/2 based on the turbulent Reynolds number and the nature of the phase producing interfacial turbulence. A similar approach has been recently proposed, but for the Pr exponent ‘n’ by McKenna & McGillis (2004) to characterize the condition of the surface ( $n = 2/3 - 1e-p$ , with exponent ‘p’ made dependent on the state of the surface, i.e. including surfactant effects). In the original work of Theophanous et al (1976), the threshold between small eddy and large eddy is about  $Re_t = 500$ , taken in the liquid bulk considering that turbulence is generated underneath the free surface due to upwelling actions. In various industrial applications, however, turbulence could be generated at the interface due to the imposed gas-side shear, in which case the turbulence Reynolds number should be taken right at the interface, where  $Re_t$  could be ten times larger than in the core. More precisely, the model is implemented in TransAT such as ‘m = -1/2’ for  $Re < 3'000$ , and ‘m = -1/4’ for  $Re > 15'000$ , with a linear match between these two limits. The question of selecting the right turbulent Reynolds number is posed in the ITM context, too, albeit the concept provides a wider degree of freedom compared to the two-fluid model which compromises the determination of near-interface turbulence properties (in particular  $U\tau$ ) because of interface smearing. In TransAT, the turbulence Reynolds number can be defined in various ways, depending on the model employed and the nature of the flow:

$$Re_t = \frac{k^2}{\nu \varepsilon}; \quad Re_y = \frac{|\Phi| \sqrt{k}}{\nu}; \quad y^+ = \frac{|\Phi| U_\tau}{\nu} \quad (21)$$

The first form of Reynolds number,  $Re_t$ , should be taken in the core flow of the turbulence-generating phase; with the associated turbulence scales determined as:

$$L_t \equiv k^2 / \varepsilon u_t, \quad \text{with} \quad u_t = \min \left( |u|, C_\mu^{1/4} k^{1/2} \right) \quad (22)$$

Alternatively, the second form could be taken, which requires the distance to the interface as the length scale. The velocity scale is now made proportional to TKE. The last form invokes the shear at the interface which can precisely be determined using ITMs ( $\phi$  is a distance to the interface). An order of magnitude estimation of these numbers in practical applications is:  $Re_t \sim 10^2 - 3 \sim 10^{-3} Re$  in the bulk (Theophanous et al., 1976). At the interface,  $Re_y \sim 10 Re_t$ .



## References

- S. Banerjee, D. Lakehal and M. Fulgosi, "Surface divergence models for scalar exchange between turbulent streams", *International journal of multiphase flow*, 30(7), 963-977 (2004).
- R. Higbie, "The rate of absorption of a pure gas into a still liquid during short periods of exposure", *Trans. Amer. Inst. Chem. Eng.* 31, 365-388 (1935).
- R. I. Eddington and D. B. R. Kenning, "The Effect of Contact Angle on Bubble Nucleation", *Int. J. Heat Mass Transfer*, 22, pp. 1231-1236 (1979).
- D. Lakehal, M. Meier, and M. Fulgosi, "Interface Tracking towards the Direct Simulation of Heat and Mass Transfer in Multiphase Flows," *Int. J. Heat & Fluid Flow*, 23, 242-257 (2002)
- D. Lakehal, "LEIS for the prediction of turbulent multifluid flows applied to thermal-hydraulics applications", *Nuclear Engineering and Design*, 240(9), 2096-2106 (2010).
- D. Lakehal, M. Fulgosi and G. Yadigaroglu, "Direct numerical simulation of condensing stratified flow", *Journal of Heat Transfer*, 130, 021501 (2008).
- D. Lakehal, M. Fulgosi, S. Banerjee and G. Yadigaroglu, "Turbulence and heat exchange in condensing vapor-liquid flow", *Physics of Fluids*, 20, 065101 (2008).
- P. Liovic, D. Lakehal, "Interface-turbulence interactions in large-scale bubbling processes", *Int. J. Heat & Fluid Flow*, 28, 127-144 (2007).
- P. Liovic, D. Lakehal, "Multi-Physics Treatment in the Vicinity of Arbitrarily Deformable Fluid-Fluid Interfaces", *J. Comp. Physics*, 222, 504-535 (2007).
- S. P. McKenna and W. R. McGillis, "The role of free-surface turbulence and surfactants in air-water gas transfer", *International journal of heat and mass transfer*, 47(3), 539-553 (2004).
- E. Krepper, and R. Rzehak. "CFD for subcooled flow boiling: Simulation of DEBORA experiments", *Nuclear Engineering and Design*, 241(9), pp. 3851-3866 (2011).
- N. Kurul, and M. Z. Podowski, "Multidimensional Effects in Forced Convection Subcooled Boiling", *Proc. of 9th Int. Heat Transfer Conference, Jerusalem, Israel*, 21-26 August (1990).
- M. Sussman, P. Smereka, S. Osher, "A Level-Set Approach for Computing Solutions to Incompressible Two-Phase Flow," *J. Comput. Phys.* **114**, 146-159 (1994).
- T.G. Theophanous, R.N. Houze and L.K. Brumfield, "Turbulent mass transfer at free gas-liquid interfaces, with applications to open-channel, bubble and jet flow", *Int. J. Multiphase Flow*, 19, 613-623 (1976).
- L. Vyskocil and J. Macek, "Boiling Flow Simulation in NEPTUNE CFD and FLUENT Codes", *XCFD4NRS, Grenoble, France*, 10 - 12 Sep. (2008).
- H. C. Ünal, "Maximum bubble diameter, maximum bubble growth time and bubble growth rate during subcooled nucleate flow boiling of water up to 17.7MW/m<sup>2</sup>", *Int. J. Heat Mass Transfer* 19, pp. 643-649, (1976).